Oligothiophene molecular wires at graphene-based molecular junctions

Tingwei Gao, Chunhui He, Chenguang Liu, Yinqi Fan, Cezhou Zhao, Chun Zhao, Weitao Su, Yannick J Dappe, Li Yang

PCCP

PAPER

View Article Online
View Journal | View Issue

Cite this: *Phys. Chem. Chem. Phys.*, 2021, **23**, 21163

Oligothiophene molecular wires at graphene-based molecular junctions†

Tingwei Gao,‡[ab] Chunhui He,‡[ab] Chenguang Liu,[a] Yinqi Fan,[ab] Cezhou Zhao,[c] Chun Zhao,[c] Weitao Su,[d] Yannick J. Dappe[e] and Li Yang *[ab]

Received 4th July 2021,
Accepted 26th August 2021

DOI: 10.1039/d1cp03050g

rsc.li/pccp

The use of graphene as a new type of electrode at molecular junctions has led to a renewal of molecular electronics. Indeed, the symmetry breaking induced by the graphene electrode yields different electronic behaviors at the molecular junction and in particular enhanced conductance for longer molecules. In this respect, several studies involving different molecular backbones and anchoring groups have been performed. Here in the same line, we consider oligopthiophene based hybrid gold–graphene junctions and we measure their electrical properties using the STM-*I*(*s*) method in order to determine their attenuation factor and the effect of specific anchoring groups. The results are supported by density functional theory (DFT) calculations, and exhibit a similar behavior to what is observed at alkane-based junctions.

Introduction

In 1988, Aviram *et al.*[1] first used a scanning tunnelling microscope (STM) to observe the *I*–*V* characteristics of a single molecule. Since then, extensive work towards many aspects of molecular electronics has been performed.[2] Indeed, understanding the electronic transport in a molecular junction is a very complex task[3] since many different factors influence the electronic conductance, such as molecular level alignment, coupling to the electrodes, molecular symmetries, *etc.*

Obviously, the first parameter to be considered in a molecular junction is the nature of the molecular backbone. As such, a common way to optimise the charge transport efficiency is to use π-conjugated systems, which are known as highly conductive molecular wires. In particular, oligothiophenes (OTs) are widely considered among various π-conjugated molecules for molecular devices due to their chemical stability, optoelectronic properties and synthetic versatility.[4,5] Also the α-position (a carbon atom bonded to a functional group) and β-position (the carbon atom next to the α carbon) of oligothiophenes are interesting linkers to modulate the electronic state. Several research studies showed that oligothiophene molecules exhibit specific electrical properties. For example, Kergueris *et al.*[6] studied bisthiolterthiophene between gold electrodes using the mechanically controllable break junction (MCBJ) method, and observed that changing the distance between the two gold electrodes induced switching between different kinds of *I*–*V* curves. Capozzi *et al.*[4] used the STM-break junction (STM-BJ) technique to investigate the length-dependent conductance of OTs (comprising 1–6 thiophene rings) with methyl sulfide end groups. They found that the conductance did not follow a clear exponential decay with the increasing number of thiophene rings, and they attributed this to different conformers at molecular junctions (MJs). Xu *et al.*[7] also observed an unusual situation for oligothiophene with –SH at the extremities: Au/alpha-quaterthiophene/Au junctions with 4 thiophene rings is more conductive (7.5×10^{-5} G_0) than the Au/alpha-terthiophene/Au junctions with 3 thiophene rings (2.8×10^{-5} G_0). This anomalous conductance was attributed to a closer location to the Fermi level of the quaterthiophene HOMO level. Another interesting example was reported by Yamada and co-workers. They observed an extremely low decay constant of 0.1 $Å^{-1}$ for the length dependence of the conductance of oligothiophene molecules terminated with a thiocyanate group, making it a good molecular wire candidate for long–range conduction.[8]

Besides, anchoring groups between molecules and electrodes are one of the main studied factors to understand the transport characteristics in MJs. There are now diverse examples of anchoring groups revealing the fundamental charge transport across the MJs. In 2003, Xu and Tao first reported the successful formation of MJs using the STM-BJ method.[9] The decay constant

[a] *Department of Chemistry, Xi'an-Jiaotong Liverpool University, Suzhou, 215123, China. E-mail: li.yang@xjtlu.edu.cn*
[b] *Department of Chemistry, University of Liverpool, Liverpool, L69 7ZD, UK*
[c] *Department of Electrical and Electronic Engineering, Xi'an-Jiaotong Liverpool University, Suzhou, 215123, China*
[d] *College of Materials and Environmental Engineering, Hangzhou Dianzi University, Hangzhou, 310018, China*
[e] *SPEC, CEA, CNRS, Université Paris-Saclay, CEA Saclay, Gif-sur-Yvette Cedex 91191, France*

† Electronic supplementary information (ESI) available. See DOI: 10.1039/d1cp03050g

‡ These authors have equally contributed to this paper.

or attenuation factor (β), describing the efficiency of electron transport, β = 1.0 ± 0.1 per carbon atom was calculated for hexanedithiols, octanedithiols and decanedithiols. This method can be also applied to other bifunctional molecules without a linker such as 4,4′ bipyridine (44BP). Interestingly, 44BP-gold single-molecule junctions achieved reversible binary switching by mechanical control of successive compression and elongation.[10] This switching mechanism was explained by the intrinsic N lone pair in the pyridine–gold link. A similar well-defined electronic coupling of the N lone pair to the Au has been linked to significantly less variation from junction to junction at the diamine molecule–Au junctions when compared with diisonitrile and dithiol–Au junctions.[11] Using gold metal electrodes, Venkataraman and co-workers found that the donor–acceptor bonds between ligands (amines, dimethyl phosphines, or methyl sulfides) and gold result in selective bonding. The strong π-back-donation in the phosphines corresponds to the increased conductivity seen for phosphines compared with methyl sulfides and amines.[12] An intuitive review by Wandlowski and co-workers[13] summarized the anchoring group effect on diaryloligyne, oligophenyleneethynylene (OPE) and/or alkane MJs composed of dihydrobenzo[*b*]thiophene (BT), 5-benzothienyl analogue (BTh), thiol (SH), pyridyl (PY), amine (NH_2), cyano (CN), methyl sulphide (SMe), nitro (NO_2) and other anchoring groups.

Finally, the nature of the electrode also plays an important role in the electronic transport through a molecular junction. However, despite significant progress in the past few decades, the most prevalently used contact is still gold metal. Gold electrodes are stable under ambient conditions and are readily available through mature fabrication techniques. Only very recently, the use of other electrodes has revealed new insights for understanding electrode–molecule interactions. In 2015, Brooke and co-workers reported that 44BP single molecule junctions with Ni contacts have a higher conductance than the analogous Au-based devices.[14] Rectification behaviour was observed in a hybrid device structure with amine-terminated oligophenyls sandwiched between a gold tip and a graphite substrate.[15] Cao *et al.* used graphene electrodes to create ''robust and identical molecular transport junctions'' using a lithographic method.[16] To further prove the effectiveness of their junctions, they capped molecules with amino groups to construct graphene/molecule/graphene symmetric junctions, which showed excellent reproducibility and stability. In a previous study[17] we have constructed a hybrid gold–molecule–graphene junction, considering a gold electrode at one side and a graphene electrode at the other side of the junction to form an asymmetric junction. As a result, we have obtained a much lower decay constant (β = 0.37 Å^{-1}) with respect to a standard gold–molecule–gold junction ($\beta \sim$ 1.0 Å^{-1}), leading to a more conductive MJ for longer alkane chains. Similar results have been obtained for different anchoring groups,[18] but not for other molecular backbones. For example, the use of polyphenyl chains with graphene electrodes did not bring any difference in the attenuation factor.[19] In this work, we consider oligothiophenes as molecular backbones to build hybrid gold–molecule–graphene junctions and we measure their electrical properties using the STM-*I*(*s*) method.[20] The aim of the study is twofold. First, we consider thiophene molecules with an increasing number of thiophene rings (n = 4, 6, and 8) in order to determine the corresponding attenuation factor. Moreover, we do not consider any anchoring group here, as we are interested in the attenuation factor of the pristine molecule. Second, we consider oligothiophenes of the same length (terthiophenes) and we probed the effect of different anchoring groups on the conductance. Namely we have used unusual anchoring groups like –Br and –CHO groups (5,5″-dibromo-2,2′:5′,2″-terthiophene, 2,2′:5′,2″-terthiophene-5,5″-dicarboxaldehyde and 5″-bromo-2,2′:5′,2″-terthiophene-5-carboxaldehyde) for their particular electronic withdrawing properties. Density functional theory (DFT) calculations support and help in interpreting the experimental results. These results are then analyzed in the light of our previous studies on alkane[17,18,21–24] or phenyl chains[19] using gold and graphene electrodes, in particular with respect to the attenuation factor and molecular conductance.

Experimental

The gold STM tips used in this experiment were prepared by an electrochemical etching process with gold as electrodes and hydrochloric acid in ethanol ($HCl : C_2H_5OH$ = 1 : 1) as the electrolyte.[25] Briefly, a gold ring of 1 cm diameter made by using a gold wire (ϕ = 0.25 mm; purity 99.99%) purchased from Tianjin Lucheng was immersed just below the liquid level of the etchant to act as an anode. Then a gold tip, acting as a cathode, was inserted vertically into the middle of the ring with one end into the electrolyte to about 0.5 cm. Then 5 V of electric power was applied to the system and the surroundings of the anode started bubbling. When the current decreased to zero, the power was turned down and the gold tip with a pointed head was formed. The prepared gold tip was removed from the etching apparatus and cleaned several times with alcohol and distilled water.

Several solvents were used to dissolve oligothiophene including mesitylene (98%, Nine-Dinn Chemistry, Shanghai, Co., Ltd), 1,2,4-trichlorobenzene (99%, Shanghai Macklin Biochemical Co., Ltd) and toluene (98%, Nine-Dinn Chemistry, Shanghai, Co., Ltd). Tetrahydrofuran (THF) with toluene in 2 : 8 and 5 : 5 ratios was also used for dissolving oligothiophene. In terms of solubility of oligothiophene, 1,2,4-trichlorobenzene (TCB) was found to be the best choice. In order to maintain the experimental conditions as identical as possible, TCB was used to dissolve all the molecules studied. The concentration for all the solution was about 10 mmol L^{-1}, except for alpha-sexithiophene and alpha-octothiophene (less than 10 mmol L^{-1}) due to the low solubility.

Molecules used for preparing MJs in the experiment are mainly purchased from TCI Chemicals (used as received) and listed in Table 1 below. The spectroscopic investigation of the purity and composition of all the molecules is presented in the ESI.†

Conductance measurements were carried out following the STM *I*(*s*) method reported by Haiss *et al.*[20] A liquid cell was used

Table 1 Molecules used to build molecular junctions

Name	Molecular formula	Structure	Molecular length (nm)	Abbreviation
Alpha-quaterthiophene	$C_{16}H_{10}S_4$	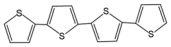	1.15	OT4
Alpha-sexithiophene	$C_{24}H_{14}S_6$	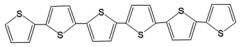	1.90	OT6
Alpha-octothiophene	$C_{32}H_{18}S_8$	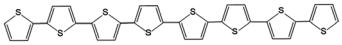	2.64	OT8
5,5″-Dibromo-2,2′:5′,2″-terthiophene	$C_{12}H_6Br_2S_3$	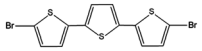	1.37	OT3a
2,2′:5′,2″-Terthiophene-5,5″-dicarboxaldehyde	$C_{14}H_8O_2S_3$	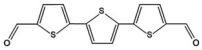	1.34	OT3b
5″-Bromo-2,2′:5′,2″-terthiophene-5-carboxaldehyde	$C_{13}H_7BrOS_3$	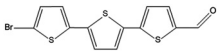	1.36	OT3c

for all the measurements. A few layer graphene deposited on a Ni substrate purchased from Graphene Supermarket, US, was glued on the sample plate by the silver gel 24 hours before each experiment. This procedure ensures a good electrical contact between the graphene and the metal sample plate. During the measurement, 1 to 2 drops of the target molecule with TCB were added into the cell. Consistent parameters were used for every measurement, typically a 300 mV sample bias, 4 nm ramp size and 50 nA current setpoint. Operating in the ramp mode, the gold tip approaches and withdraws away from the graphene. A large number of $I(s)$ curves (more than 20 000 for each molecule) containing current steps were obtained. According to the position of the plateaus, the original $I(s)$ curves were segmented with 5 nA interval equally based on the current set point. The curves from bins with the largest and the second largest numbers were then selected and converted into conductance values to obtain a one-dimensional (1D) electrical conductance histogram. About 500 selected curves containing characteristic plateaus of every MJs are included to calculate the most dominant conductance values.

In order to interpret the experimental results and to understand the physical mechanisms, we have performed DFT calculations. To this end, we have used the very efficient localized-orbital basis set DFT code Fireball.[26] In this approach, a self-consistent version of the Harris–Foulkes local density approximation (LDA) functional[27,28] is used, instead of the traditional Kohn–Sham functional based on electronic density. Hence, the potential is calculated by approximating the total charge by a superposition of spherical charges around each atom. In this framework, self-consistency is achieved over the occupation numbers through a modified version of the Harris functional.[29] Besides, the LDA exchange–correlation energy is calculated using the efficient multi-center weighted exchange–correlation density approximation (McWEDA).[30,31] Optimized numerical basis sets[32] have been used for structural optimization and conductance calculation for all the MJs, namely alpha quater-, sexi- and octo-thiophene, as well as tert-hiophene with Br and CHO groups, similarly to what have been used in previous work on oligothiophenes.[33] The gold tip has been modelled by a pyramid of 35 Au atoms, terminating in a single apex.[18] We have considered a supercell of 5 × 5C atoms in the XY plane for the graphene monolayer, on top of which we have set a molecule of defined length in the z direction, terminated by a connection with the Au pyramidal tip. The whole geometry has been optimized with Fireball until the forces reached a value below 0.05 eV Å^{-1}. In a second step, we have used a nonequilibrium Keldysh–Green formalism, which takes multiple scattering into account to determine the conductance of the MJs.[34]

Results and discussion

We first measured the gold–oligothiophene–graphene junctions (first group). As shown in Fig. 1a, clear steps are observed in the curves and the conductance of Au/OT6/graphene junctions is around $6.5 \times 10^{-4}\ G_0$ to $1.0 \times 10^{-3}\ G_0$. About 500 $I(s)$ curves were selected to plot a 1D histogram to find the dominant location of the conductance peak. There is only one peak in the histogram (Fig. 1b), which indicates that the conductance of OT6 is $8.8 \times 10^{-4}\ G_0$ by using a Gaussian fit of this peak. These selected $I(s)$ curves were also used to plot a two-dimensional (2D) histogram as shown in Fig. 1c and the red part around $6.5 \times 10^{-4}\ G_0$ to $1.0 \times 10^{-3}\ G_0$ agreed well with the original plateau curves in Fig. 1a, indicating the most probable configuration being formed under our experimental conditions.

As shown in Fig. 2a, it is clear that the conductances of the first group graphene-based MJs (n = 4, 6, and 8) decrease when the molecular length increases, in good agreement with the results reported by Zhang *et al.*[18] For example, the conductance of Au/OT4/graphene junctions is around $1.7 \times 10^{-3}\ G_0$ to $1.9 \times 10^{-3}\ G_0$.

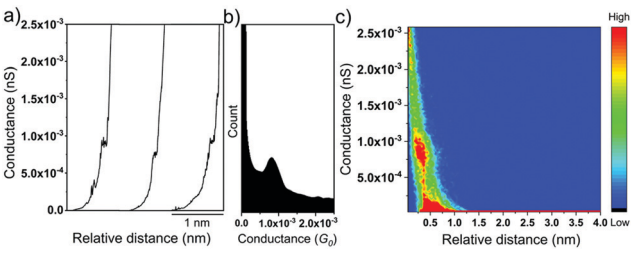

Fig. 1 (a) Typical $I(s)$ curves of Au/OT6/graphene junctions collected by the $I(s)$ method at 300 mV; (b) the one-dimensional (1D) histogram of single molecule conductance of OT6 constructed from about 500 curves; (c) the two-dimensional (2D) histograms of the conductance of OT6.

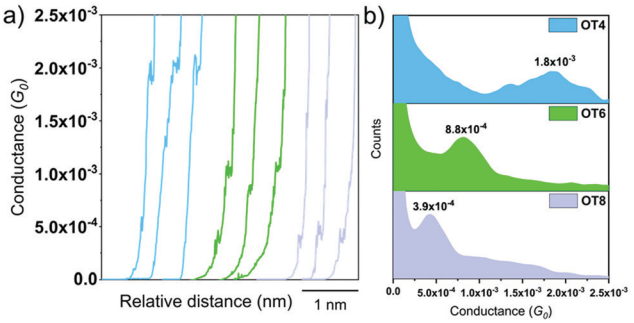

Fig. 2 (a) Typical *I*(*s*) curves and (b) 1D histograms of Au/OT4/graphene MJs (blue), Au/OT6/graphene MJs (green) and Au/OT8/graphene MJs (purple).

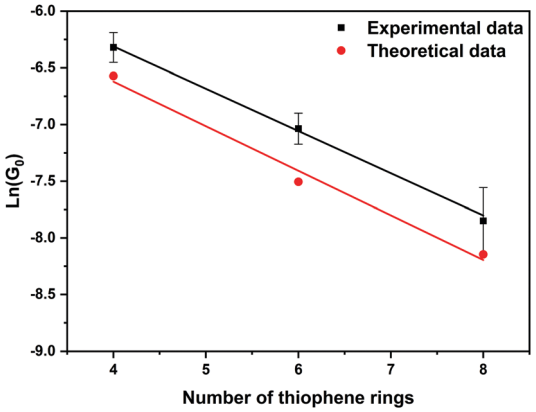

Fig. 3 Linear fitting of the conductance of Au/oligothiophene/graphene junctions *versus* the number of thiophene rings. The error bars are derived from the full width half maximum (FWHM) of the Gaussian peak fitting of 1D histograms.

When the number of thiophene rings increases from 4 to 6, the conductance of Au/OT6/graphene junctions decreases to around 7.8 × 10^{-4} G_0 to 1.0 × 10^{-3} G_0. Fig. 2b shows the 1D conductance histogram of the Au–oligothiophene–graphene molecular junction (OT4: blue, OT6: green and OT8: purple) by using around 500 curves of each molecule. Interestingly, the conductance peaks appear sharper as the wire becomes longer. Our results show an unusual conformational effect in these hybrid graphene MJs, which has been previously reported that the conductance distribution became broader with the increasing molecular length of OTs terminated by methyl sulfide.[4] The authors claimed that the rotational freedom is more restricted for shorter molecules and adding extra thiophene units yields extra disorder to the system, resulting in the conformation of MJs varying from junction to junction. In our case, the planar structure of graphene with more neighbouring atoms probably places more strain to restrict the conformation and the degree of freedom, resulting in less junction-to-junction variation. From these histograms, we can deduce that the conductance of these three MJs with different thiophene rings (n = 4, 6, and 8) is 1.8 × 10^{-3} G_0, 8.8 × 10^{-4} G_0 and 3.9 × 10^{-4} G_0, respectively. A much higher conductance for OT4 was observed compared to OT6 and OT8. This behavior agrees with the results reported by Capozzi *et al.*[4] Wu and co-workers[35] also measured the carbon chain–graphene junctions and found that the thermoelectric performance of MJs is very sensitive to the length of the molecular wire and an odd–even characteristic with the increase of chain length was reported. Further plotting the data as a linear fit to the conductance points gives a decay constant of β = 0.39 Å^{-1} from the slope shown in Fig. 3. This lower decay constant is consistent with previously reported decay constants (0.1–0.4 Å^{-1})[4,8,36] for π-conjugated oligothiophenes. Our results show as expected that the conductance exponentially decays with an increasing molecular length similarly to what was obtained by Zhang[18] and He[22] on alkanedithiol and alkanediamine chains. Indeed, the exponential decay of the conductance is the full expression of the non-resonant tunnelling mechanism here, which is similar to the electronic transport properties of the Au/*n*-alkanedithiol/graphene junctions.[18] Since the couplings in both systems lead to similar electronic barriers, and consequently a similar attenuation factor, it is expected that for equivalent lengths, the conductance will evolve similarly. As shown in Fig. S13 (ESI†), the conductance values for Au/*n*-alkanedithiol/graphene junctions are much smaller for Au/OT/graphene junctions with a similar length. This is explained by the effect of conjugated oligothiophenes *versus* a nonconjugated alkane molecular backbone on electron transmission.[37] Another reason is related to the contact resistance of the junction, *i.e.* the prefactor of the exponential behavior. This contact resistance depends on the coupling to the electrode (which is different here due to different atoms in contact) and the way the molecule is connected at the atomic level. By extending the fit of experimental data of Fig. 3 to the zero thiophene ring, the resulting intercept of the Y axis represents the contact resistance (1.5 MΩ) of Au/OT/graphene MJs. This value is smaller than that obtained for Au/*n*-alkanedithiol/graphene junctions (3.9 MΩ) in our previous study[21] and much higher than that obtained for Au/Au symmetric contacts processing two Au–S–alkane contacts (27 kΩ). This difference again highlights the fact that the important advantage in the use of graphene electrodes for MJs lies in the weak interaction with the molecular target, resulting in the intrinsic electronic properties of the molecule remaining largely unaffected by the contact with the electrode, contrary to a metallic electrode where there is a strong hybridization at the interface.

In order to support these experimental results, we have performed DFT calculations to determine the electronic transport properties of oligothiophene MJs as a function of the number of thiophene rings. The corresponding optimized atomic configurations are represented in Fig. 4a. Table 2 presents the experimental and the corresponding theoretical conductance results for Au/oligothiophene/graphene. The theoretical conductance of the MJs at the Fermi level is calculated using a formula of $G = T(E)$ from the electronic transmission plot as seen in Fig. 4b. A comparative analysis of the experimental (black) and theoretical (red) results is also included in Fig. 3. Despite some discrepancy, the general trend is in good agreement with a similar β value of the simulation. From the calculated electronic transmissions $T(E)$ in the vicinity of the Fermi level, an important feature that can be observed on the calculated

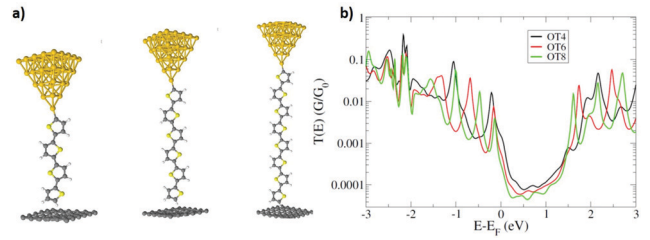

Fig. 4 (a) Atomic representation of the oligothiophene based MJs used for the DFT calculations. (b) Corresponding calculated electronic transmissions.

transmissions is the position of the highest occupied molecular orbital (HOMO) level for each junction, around 0.2 eV from the Fermi level. The proximity of the HOMO level to the Fermi level indicates a general electronic donor trend of the thiophene based molecular junction. This is in good agreement with a previous STM study on polythiophene lifted from a gold surface. In that case, the two gold electrodes at each side of the molecule cancel the shift of the HOMO position.[33] Interestingly, the HOMO resonance at 0.2 eV is very similar to the one obtained in the case of alkanedithiol MJs.[18] According to Simmond's model[38] applied in the alkanedithiol case, the attenuation factor varies as the square root of the energy difference between the Fermi and the HOMO level. Therefore, this similar value of the energy difference justifies the similar value of the attenuation factor obtained here, in good agreement with the experiments.

In this respect, oligothiophene graphene-contact MJs seem to behave very similarly to alkane-based graphene hybrid MJs, even though we have not performed a comparison with the same anchoring groups. This behavior might be expected as the electronic transport properties of these systems are driven by a balance between strong covalent bonds at the gold electrode and weak van der Waals bonds at the graphene interface. Note that this effect has also been observed for the alignment of the projected density of states (PDOS) under bias in asymmetric junctions.[39,40] This has obviously an influence on the contact resistance and also on the electronic transport in the junction through a reduction of the attenuation factor. This has been explained in our previous studies,[17,18] and the obtained behaviour is very similar to what we obtained at the alkanedithiol junction[18] with a small electronic barrier between the HOMO and the Fermi level. This result is in contrast to measurements of OT-based MJs using Au electrodes, suggesting that the conductance of a molecule is highly sensitive to the molecule–electrode contact. It is well known that saturated alkanes with larger HOMO and lowest unoccupied molecular orbital (LUMO) gaps have larger decay constants of about 1 $Å^{-1}$, while lower decay constants are observed for more conducting unsaturated π-conjugated molecules using Au contacts. For instance, the decay constants of 0.211 $Å^{-1}$ for thiophenedithiol and 0.264 $Å^{-1}$ for thiophenediamine were reported.[36] Kuang and co-workers claimed almost no decay ($\beta < 0.001$ $Å^{-1}$) conductance of single porphyrin oligomer wires at long range (> 6 nm).[41] These types of molecular wires with nonlinear backbones also show interesting negative differential conductance in resonant transport.[42] The analysis shows that the difference is attributed not only to the intrinsic band gap of the molecular wire, but also to the charge transfer at the interface. Ohto *et al.* used different computational methods to calculate the decay constant of the *trans*-OTs. They obtained values ranging from 0.14 to 0.19 $Å^{-1}$.[43] In another set of examples using iodide-terminated oligothiophene molecules, simple exponential length dependence was not followed for $n = 1$, 2, and 3 and it is resumed for longer molecules ($n > 4$) with a β value of 0.32 $Å^{-1}$. They attributed the observation to a transition in the molecule–electrode binding geometry as the molecular length increases, which highlights the importance of electrode–molecule coupling *via* the π-electrons.[44]

We turn our attention now to the influence of anchoring groups on terthiophene-based MJs. This system has been already studied using standard Au electrodes,[4,7,36] while to our best knowledge no data were found for using hybrid graphene electrodes. Here, in contrast to well-known anchoring groups (–SH, $–NH_2$, COOH, *etc.*), unusual anchoring groups (–Br and –CHO) have been chosen following a long-term goal in the understanding of the respective influence of molecular backbones, anchoring groups and electrodes on the electronic transport properties of MJs. The interest in –Br and –CHO groups lies in their electron-withdrawing property, which moves a molecular level closer to the Fermi level, enhancing the charge transport. It was reported that the interaction of electron withdrawing molecules with graphene is stronger than that of electron donating molecules.[45] Venkataraman and co-workers showed that when using gold as electrodes, electron-donating substituents drive the occupied molecular orbitals up and increase the junction conductance, while electron-withdrawing substituents behave oppositely.[46] Such difference derived from different electrodes is interesting. It is clear that the use of graphene electrodes introducing asymmetric elements to the MJs might reveal new insight and inspire new design for the fabrication of high-performance molecular devices. Also, pure spin current and a spin-dependent Seebeck coefficient were observed in cobaltocene-based molecular junctions.[47] It is expected that such metallocence-dimer-based MJs have potential in promising spin thermoelectric devices and energy-saving devices. Fig. 5a shows the typical $I(s)$ curves of OT3a (grey), OT3b (yellow) and OT3c (black) bridged between the Au tip and graphene substrate. To better illustrate the change of conductance with anchoring groups, stacked 1D histograms were plotted with

Table 2 Conductance values for molecules with graphene bottom electrodes

Molecular junctions	Au/OT4/graphene	Au/OT6/graphene	Au/OT8/graphene	Au/OT3a/graphene	Au/OT3b/graphene	Au/OT3c/graphene
Experimental data (G_0)	1.8×10^{-3}	8.8×10^{-4}	3.9×10^{-4}	1.3×10^{-3}	1.2×10^{-3}	1.4×10^{-3}
Theoretical data (G_0)	1.4×10^{-3}	5.5×10^{-4}	2.9×10^{-4}	1.4×10^{-3}	1.1×10^{-3}	1.3×10^{-3}

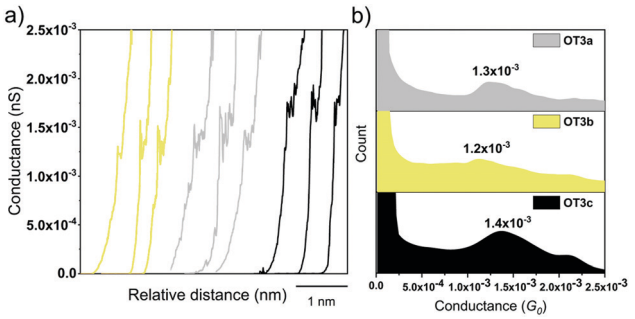

Fig. 5 (a) Typical *I*(*s*) curves and (b) 1D histograms of Au/OT3a/graphene MJs (grey), Au/OT3b/graphene MJs (yellow) and Au/OT3c/graphene MJs (black).

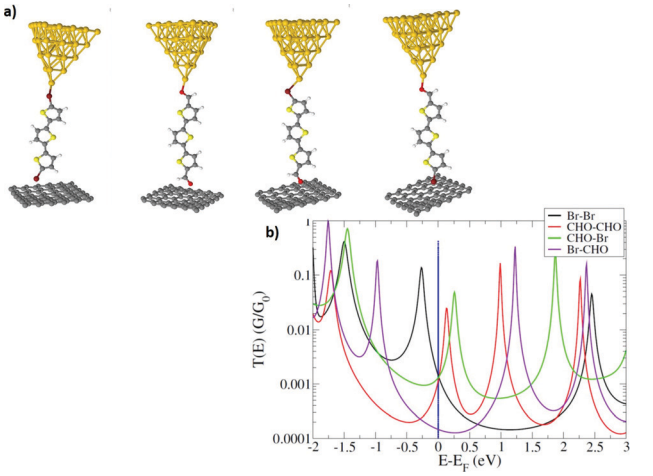

Fig. 6 (a) Atomic representation of the hybrid terthiophene based MJs, with –Br and –CHO anchoring groups, used for DFT calculations. (b) Corresponding calculated electronic transmission spectra, in which the vertical blue line stands for the Fermi level.

the same conductance and counts scale as shown in Fig. 5b. For each conductance histogram, only one single peak dominates. The following conductance values have been recorded for the second group of MJs: 1.3×10^{-3} G_0 (Au/OT3a/graphene), 1.2×10^{-3} G_0 (Au/OT3b/graphene) and 1.4×10^{-3} G_0 (Au/OT3c/graphene), respectively. In Fig. 5b we can see that the conductance of OT3c is the highest (black) and the conductance of OT3b (yellow) is the lowest. These values indicate that asymmetric terminated ending groups induce an enhanced electrical conduction for π-conjugated oligothiophenes with the Au/graphene system, while previously the conductance value for alkane chains terminated with thiol and carboxylic acid is between the symmetric anchoring groups with the Au/graphene system.[24] Although OT3a, OT3b and OT3c have different substitute groups on the thiophene ring, the molecular length of them is essentially identical (See the data in Table 1) and we expect that the conductance evolves similarly. The conductance variation shown in Fig. 5b again emphasises the importance of using a graphene electrode here. Recently Hong and co-workers presented that the charge-transport ability through the single stacking junctions based on thiophene units has no obvious dependency on the conjugation pattern. Thiophene molecules with one –SMe terminus and chlorine or bromine as another terminus, and fused-ring thiophenes showed very similar conductance values centered at $10^{-4.0}$ G_0.[48]

In order to interpret the experimental results, in the same manner as for the attenuation factor determination, we have performed DFT calculations on terthiophene-based MJs using –Br and –CHO anchoring groups at both ends. However, in the case of mixed anchoring groups, the question arises of where is the Br and where is the CHO group? Indeed, in the present experiments, we cannot identify whether the Br or the CHO group of the terthiophene molecule binds on graphene since we have no experimental evidence for a preferential adsorption of a specific group. Also, these specific connections are of paramount importance, since the coupling to the electrodes is very much dependent on the anchoring groups for symmetry reasons, as shown in our previous studies on alkanedithiol and alkanediamine molecular junctions.[17,18] Hence, we have considered theoretically the two possibilities and therefore, the four different junctions are represented in Fig. 6a.

The characteristic molecular shape when the –Br is connected to the gold electrode is very similar to that in connection with a $-NH_2$ group,[49] which induces a curvature in the molecular junction. In Fig. 6b, we present the corresponding calculated electronic transmission spectra. We then can observe very different behaviors according to the different groups. Indeed, for the Br–Br junction, the electronic transport is driven by the HOMO level, as the closest molecular level to the Fermi level, which means that we retain the donor character of the pristine thiophene. Oppositely, for the CHO–CHO junction, the LUMO level drives the electronic transport, as it is the closest level to the Fermi level, which means that the molecule is now an acceptor. These features can be identified in the electronic transmission spectra with the corresponding resonances near the Fermi level. For these two junctions, we obtain conductances of 1.4×10^{-3} G_0 and 1.1×10^{-3} G_0, respectively, in good agreement with the experimental results (Table 2). Now considering the mixed junctions with one Br and one CHO, we obtain very different results, according to the connection of the Br to the gold or to the graphene electrode. When the –Br group is connected to gold, it seems that the acceptor and donor characters of both different anchoring groups are cancelled, which locates the Fermi level in the middle of the molecular gap. As a result, the conductance is very low and does not correspond to the experimental result. Hence, this configuration is not realistic, and we can infer that the –Br group is connected to the graphene electrode. This is probably due to a better affinity of Br on graphene upon molecular deposition. Now if we consider the last molecular junction, which connects –CHO with the gold electrode, in this case, similarly to the CHO–CHO junction, the LUMO level drives the electronic transport, and brings a conductance value of 1.3×10^{-3} G_0, very close to those of the symmetric Br–Br and CHO–CHO cases. This is also in good agreement with a previous study on an asymmetric S–COOH alkane-based molecular junction, where the electronic current takes the easiest conduction channel.[50] Indeed, each anchoring

group offers different potential conductance channels to the MJs, and here for example, the conductance is driven by the close location to the Fermi level of the LUMO, similarly to what happens in the full CHO–CHO molecular junctions.

Conclusions

To summarize, using the STM $I(s)$ method, we have measured the conductance of different oligothiophene based molecular junctions, using a gold electrode at one side and a graphene electrode at the other side. First, we have determined the attenuation factor of anchoring group-free oligothiophene junctions, and we have found that it is very similar to what is obtained for alkane chains using different anchoring groups. Second, we have considered terthiophenes with different anchoring groups like –Br or –CHO either in symmetric or asymmetric configurations. We can observe that according to the anchoring group, the electronic character of the molecules changes between the donor and acceptor. Also for the asymmetric configuration, we recover also similar results to what have been obtained for alkane chains. Finally, DFT calculations support the experimental results and allow the identification of that the –Br group connects to the graphene probably due to a better affinity compared to the –CHO group. This work opens a promising way to develop and tune oligothiophene based molecular junctions with different electronic properties.

Author contributions

Tingwei Gao and Chunhui He carried out the main experiments; Li Yang and Yannick J. Dappe wrote the manuscript and designed the experiments; Chenguang Liu and Yinqi Fan conducted other complementary experiments; Cezhou Zhao, Chun Zhao and Weitao Su analyzed the experimental results. Yannick J. Dappe developed the simulation work and analyzed the sequencing simulation data. All authors have given approval to the final version of the manuscript.

Conflicts of interest

The authors declare no competing financial interest.

Acknowledgements

This work was supported by the National Natural Science Foundation of China (NSFC Grants 21503169), the Suzhou Industrial Park Initiative Platform Development for Suzhou Municipal Key Lab for New Energy Technology (RR0140), the Key Program Special Fund in XJTLU (KSF-E-28) and the XJTLU Research Development Fund (RDF-14-02-42, RDF-16-01-33 and REF-19-01-05). The authors thank Professor Richard Nichols (University of Liverpool) for useful discussions and technical support.

Notes and references

1 A. Aviram, C. Joachim and M. Pomerantz, Evidence of Switching and Rectification by a Single Molecule Effected with a Scanning Tunneling Microscope, *Chem. Phys. Lett.*, 1988, **146**, 490–495.
2 J. C. Cuevas and E. Scheer, *Molecular Electronics: an Introduction to Theory and Experiment*, World Scientific, Singapore, 2010.
3 T. A. Su, M. Neupane, M. L. Steigerwald, L. Venkataraman and C. Nuckolls, Chemical Principles of Single-Molecule Electronics, *Nat. Rev. Mater.*, 2016, **1**, 16002.
4 B. Capozzi, E. J. Dell, T. C. Berkelbach, D. R. Reichman, L. Venkataraman and L. M. Campos, Length-Dependent Conductance of Oligothiophenes, *J. Am. Chem. Soc.*, 2014, **136**, 10486–10492.
5 I. F. P. Perepichka and F. Dmitrii, *Handbook of Thiophene-Based Materials: Applications in Organic Electronics and Photonics*, Wiley, Chichester, U.K., 2009.
6 C. Kergueris, J. P. Bourgoin, S. Palacin, D. Esteve, C. Urbina, M. Magoga and C. Joachim, Electron Transport through a Metal–Molecule–Metal Junction, *Phys. Rev. B: Condens. Matter Mater. Phys.*, 1999, **59**, 12505–12513.
7 B. Q. Xu, X. L. Li, X. Y. Xiao, H. Sakaguchi and N. J. Tao, Electromechanical and Conductance Switching Properties of Single Oligothiophene Molecules, *Nano Lett.*, 2005, **5**, 1491–1495.
8 R. Yamada, H. Kumazawa, T. Noutoshi, S. Tanaka and H. Tada, Electrical Conductance of Oligothiophene Molecular Wires, *Nano Lett.*, 2008, **8**, 1237–1240.
9 B. Q. Xu and N. J. Tao, Measurement of Single-Molecule Resistance by Repeated Formation of Molecular Junctions, *Science*, 2003, **301**, 1221–1223.
10 S. Y. Quek, M. Kamenetska, M. L. Steigerwald, H. J. Choi, S. G. Louie, M. S. Hybertsen, J. B. Neaton and L. Venkataraman, Mechanically Controlled Binary Conductance Switching of a Single-Molecule Junction, *Nat. Nanotechnol.*, 2009, **4**, 230–234.
11 L. Venkataraman, J. E. Klare, I. W. Tam, C. Nuckolls, M. S. Hybertsen and M. L. Steigerwald, Single-Molecule Circuits with Well-Defined Molecular Conductance, *Nano Lett.*, 2006, **6**, 458–462.
12 Y. S. Park, A. C. Whalley, M. Kamenetska, M. L. Steigerwald, M. S. Hybertsen, C. Nuckolls and L. Venkataraman, Contact Chemistry and Single-Molecule Conductance: a Comparison of Phosphines, Methyl Sulfides, and Amines, *J. Am. Chem. Soc.*, 2007, **129**, 15768–15769.
13 V. Kaliginedi, A. V. Rudnev, P. Moreno-Garcia, M. Baghernejad, C. Huang, W. Hong and T. Wandlowski, Promising Anchoring Groups for Single-Molecule Conductance Measurements, *Phys. Chem. Chem. Phys.*, 2014, **16**, 23529–23539.
14 R. J. Brooke, C. Jin, D. S. Szumski, R. J. Nichols, B. W. Mao, K. S. Thygesen and W. Schwarzacher, Single-Molecule Electrochemical Transistor Utilizing a Nickel–Pyridyl Spinterface, *Nano Lett.*, 2015, **15**, 275–280.

15 T. Kim, Z. F. Liu, C. Lee, J. B. Neaton and L. Venkataraman, Charge Transport and Rectification in Molecular Junctions Formed with Carbon-Based Electrodes, *Proc. Natl. Acad. Sci. U. S. A.*, 2014, **111**, 10928–10932.
16 Y. Cao, S. H. Dong, S. Liu, L. He, L. Gan, X. M. Yu, M. L. Steigerwald, X. S. Wu, Z. F. Liu and X. F. Guo, Building High-Throughput Molecular Junctions Using Indented Graphene Point Contacts, *Angew. Chem., Int. Ed.*, 2012, **51**, 12228–12232.
17 Q. Zhang, S. H. Tao, R. W. Yi, C. H. He, C. Z. Zhao, W. T. Su, A. Smogunov, Y. J. Dappe, R. J. Nichols and L. Yang, Symmetry Effects on Attenuation Factors in Graphene-Based Molecular Junctions, *J. Phys. Chem. Lett.*, 2017, **8**, 5987–5992.
18 Q. Zhang, L. L. Liu, S. H. Tao, C. Y. Wang, C. Z. Zhao, C. Gonzalez, Y. J. Dappe, R. J. Nichols and L. Yang, Graphene as a Promising Electrode for Low-Current Attenuation in Nonsymmetric Molecular Junctions, *Nano Lett.*, 2016, **16**, 6534–6540.
19 S. H. Tao, Q. Zhang, C. H. He, X. F. Lin, R. C. Xie, C. Z. Zhao, C. Zhao, A. Smogunov, Y. J. Dappe, R. J. Nichols and L. Yang, Graphene-Contacted Single Molecular Junctions with Conjugated Molecular Wires, *ACS Appl. Nano Mater.*, 2018, **2**, 12–18.
20 W. Haiss, H. van Zalinge, S. J. Higgins, D. Bethell, H. Hobenreich, D. J. Schiffrin and R. J. Nichols, Redox State Dependence of Single Molecule Conductivity, *J. Am. Chem. Soc.*, 2003, **125**, 15294–15295.
21 C. H. He, Q. Zhang, T. W. Gao, C. G. Liu, Z. Y. Chen, C. Z. Zhao, C. Zhao, R. J. Nichols, Y. J. Dappe and L. Yang, Charge Transport in Hybrid Platinum/Molecule/Graphene Single Molecule Junctions, *Phys. Chem. Chem. Phys.*, 2020, **22**, 13498–13504.
22 C. H. He, Q. Zhang, S. H. Tao, C. Z. Zhao, C. Zhao, W. T. Su, Y. J. Dappe, R. J. Nichols and L. Yang, Carbon-Contacted Single Molecule Electrical Junctions, *Phys. Chem. Chem. Phys.*, 2018, **20**, 24553–24560.
23 L. L. Liu, Q. Zhang, S. H. Tao, C. Z. Zhao, E. Almutib, Q. Al-Galiby, S. W. D. Bailey, I. Grace, C. J. Lambert, J. Du and L. Yang, Charge Transport through Dicarboxylic-Acid-Terminated Alkanes Bound to Graphene-Gold Nanogap Electrodes, *Nanoscale*, 2016, **8**, 14507–14513.
24 C. H. He, Q. Zhang, Y. Q. Fan, C. Z. Zhao, C. Zhao, J. Y. Ye, Y. J. Dappe, R. J. Nichols and L. Yang, Effect of Asymmetric Anchoring Groups on Electronic Transport in Hybrid Metal/Molecule/Graphene Single Molecule Junctions, *ChemPhysChem*, 2019, **20**, 1830–1836.
25 B. Ren, G. Picardi and B. Pettinger, Preparation of Gold Tips Suitable for Tip-Enhanced Raman Spectroscopy and Light Emission by Electrochemical Etching, *Rev. Sci. Instrum.*, 2004, **75**, 837–841.
26 J. P. Lewis, P. Jelinek, J. Ortega, A. A. Demkov, D. G. Trabada, B. Haycock, H. Wang, G. Adams, J. K. Tomfohr, E. Abad, H. Wang and D. A. Drabold, Advances and Applications in the Fireball Ab Initio Tight-Binding Molecular-Dynamics Formalism, *Phys. Status Solidi B*, 2011, **248**, 1989–2007.
27 J. Harris, *Phys. Rev. B: Condens. Matter Mater. Phys.*, 1985, **31**, 1770–1779.
28 W. M. C. Foulkes and R. Haydock, *Phys. Rev. B: Condens. Matter Mater. Phys.*, 1989, **39**, 12520–12536.
29 A. A. Demkov, J. Ortega, O. F. Sankey and M. P. Grumbach, *Phys. Rev. B: Condens. Matter Mater. Phys.*, 1995, **52**, 1618–1630.
30 P. Jelinek, H. Wang, J. P. Lewis, O. F. Sankey and J. Ortega, *Phys. Rev. B: Condens. Matter Mater. Phys.*, 2005, **71**, 2351011.
31 O. F. Sankey and D. J. Niklewski, *Phys. Rev. B: Condens. Matter Mater. Phys.*, 1989, **40**, 3979–3995.
32 M. A. Basanta, Y. J. Dappe, P. Jelínek and J. Ortega, Optimized Atomic-Like Orbitals for First-Principles Tight-Binding Molecular Dynamics, *Comput. Mater. Sci.*, 2007, **39**, 759–766.
33 G. Reecht, H. Bulou, F. Scheurer, V. Speisser, F. Mathevet, C. Gonzalez, Y. J. Dappe and G. Schull, Pulling and Stretching a Molecular Wire to Tune Its Conductance, *J. Phys. Chem. Lett.*, 2015, **6**, 2987–2992.
34 C. Gonzalez, E. Abad, Y. J. Dappe and J. C. Cuevas, Theoretical Study of Carbon-Based Tips for Scanning Tunnelling Microscopy, *Nanotechnology*, 2016, **27**, 105201.
35 D. Wu, X. H. Cao, P. Z. Jia, Y. J. Zeng, Y. X. Feng, L. M. Tang, W. X. Zhou and K. Q. Chen, Excellent thermoelectric performance in weak-coupling molecular junctions with electrode doping and electrochemical gating, *Sci. China: Phys., Mech. Astron.*, 2020, **63**, 276811.
36 G. W. Peng, M. Strange, K. S. Thygesen and M. Mavrikakis, Conductance of Conjugated Molecular Wires: length Dependence, Anchoring Groups, and Band Alignment, *J. Phys. Chem. C*, 2009, **113**, 20967–20973.
37 W. B. Chang, C.-K. Mai, M. Kotiuga, J. B. Neaton, G. C. Bazan and R. A. Segalman, Controlling the Thermoelectric Properties of Thiophene-Derived Single-Molecule Junctions, *Chem. Mater.*, 2014, **26**, 7229–7235.
38 J. G. Simmons, Generalized Formula for the Electric Tunnel Effect between Similar Electrodes Separated by a Thin Insulating Film, *J. Appl. Phys.*, 1963, **34**, 1793–1803.
39 Q. Liu, J. J. Li, D. Wu, X. Q. Deng, Z. H. Zhang, Z. Q. Fan and K. Q. Chen, Gate-controlled reversible rectifying behavior investigated in a two-dimensional MoS_2 diode, *Phys. Rev. B*, 2021, **104**, 045412.
40 Z. Q. Fan, X. W. Jiang, Z. M. Wei, J. W. Luo and S. S. Li, Tunable Electronic Structures of GeSe Nanosheets and Nanoribbons, *J. Phys. Chem. C*, 2017, **121**, 14373–14379.
41 G. W. Kuang, S. Z. Chen, W. H. Wang, T. Lin, K. Q. Chen, X. S. Shang, P. N. Liu and N. Lin, Resonant Charge Transport in Conjugated Molecular Wires beyond 10 nm Range, *J. Am. Chem. Soc.*, 2016, **138**, 11140–11143.
42 G. W. Kuang, S. Z. Chen, L. H. Yan, K. Q. Chen, X. S. Shang, P. N. Liu and N. Lin, Negative Differential Conductance in Polyporphyrin Oligomers with Nonlinear Backbones, *J. Am. Chem. Soc.*, 2018, **140**, 570–573.
43 T. Ohto, T. Inoue, H. Stewart, Y. Numai, Y. Aso, Y. Ie, R. Yamada and H. Tada, Effects of *Cis–Trans* Conformation between Thiophene Rings on Conductance of Oligothiophenes, *J. Phys. Chem. Lett.*, 2019, **10**, 5292–5296.

44 L. M. Xiang, T. Hines, J. L. Palma, X. F. Lu, V. Mujica, M. A. Ratner, G. Zhou and N. T. Tao, Non-Exponential Length Dependence of Conductance in Iodide-Terminated Oligothiophene Single-Molecule Tunneling Junctions, *J. Am. Chem. Soc.*, 2016, **138**, 679–687.

45 D. J. Late, A. Ghosh, B. Chakraborty, A. K. Sood, U. V. Waghmare and C. N. R. Rao, Molecular Charge-Transfer Interaction with Single-Layer Graphene, *J. Exp. Nanosci.*, 2011, **6**, 641–651.

46 L. Venkataraman, Y. S. Park, A. C. Whalley, C. Nuckolls, M. S. Hybertsen and M. L. Steigerwald, Electronics and Chemistry: varying Single-Molecule Junction Conductance Using Chemical Substituents, *Nano Lett.*, 2007, **7**, 502–506.

47 D. Wu, X. H. Cao, S. Z. Chen, L. M. Tang, Y. X. Feng, K. Q. Chen and W. X. Zhou, Pure spin current generated in thermally driven molecular magnetic junctions: a promising mechanism for thermoelectric conversion, *J. Mater. Chem. A*, 2019, **7**, 19037–19044.

48 X. H. Li, Q. Q. Wu, J. Bai, S. J. Hou, W. L. Jiang, C. Tang, H. Song, X. J. Huang, J. T. Zheng, Y. Yang, J. Y. Liu, Y. Hu, J. Shi, Z. T. Liu, J. C. Lambert, D. Q. Zhang and W. J. Hong, Structure-Independent Conductance of Thiophene-Based Single-Stacking Junctions, *Angew. Chem., Int. Ed.*, 2020, **59**, 3280–3286.

49 N. J. Tao, Electron Transport in Molecular Junctions, *Nat. Nanotechnol.*, 2006, **1**, 173–81.

50 M. Kiguchi, S. Miura, T. Takahashi, K. Hara, M. Sawamura and K. Murakoshi, Conductance of Single 1,4-Benzenediamine Molecule Bridging between Au and Pt Electrodes, *J. Phys. Chem. C*, 2008, **112**, 13349–13352.